IEEE Access
Multidisciplinary | Rapid Review | Open Access Journal

Date of publication xxxx 00, 0000, date of current version xxxx 00, 0000.

Digital Object Identifier 10.1109/ACCESS.2017.Doi Number

A New Soft Pneumatic Elbow Pad for Joint Assistance with Application to Smart Campus

Xifeng Gao[1], Student Member, IEEE, Yao Sun[1], Student Member, IEEE, Lina Hao[1], Member, IEEE, Hui Yang[1], Student Member, IEEE, Yang Chen[1], Student Member, IEEE, and Chaoqun Xiang[2]

[1] School of Mechanical Engineering and Automation, Northeastern University, Shenyang, 110819, China
[2] Bristol Robotics Laboratory, University of Bristol Bristol, UK

Corresponding author: L. Hao (e-mail: haolina@me.neu.edu.cn).

This work was sponsored by the National High Technology Research and Development Program of China (863 Program) under Grant No. 2015AA042302, the Joint Research of Equipment Pre-Research Program of Ministry of Education of China Foundation under Grant No. 6141A02022605 and the National Natural Science Foundation of China under Grant No. 61573093 and No. U1613205.

ABSTRACT This paper presents an assistance equipment of human elbow joint which aims to help patients who have elbow injury issues in smart campus environment. A new type of soft pneumatic elbow pad (SPEP) which adopted soft material manufacturing technology is presented. Compared with the rigid assistant equipment, the SPEP shows more comfort, smaller equipment size and convenience of wearing. Meanwhile, three different types of sensors (the air pressure sensor, bending sensor and force sensor) are used in SPEP to discover the two important characteristics which are applied. In order to verify effectiveness of the designed SPEP, two analysis methods are presented. The surface electromyogram (sEMG) signal and the root mean square (RMS) analysis are used in the first method which prove that SPEP could reduce the activity of the muscle and assist power during the elbow movement. Compared with the first method, the second method which is the model of calculation after wearing SPEP can obtain specific value of assisting power in the biceps and olecranon. Thus, the aforementioned methods illustrate the feasibility of SPEP. Finally, in order to make SPEP used in daily life, a portable backpack with the control system and the energy system is applied to the field of human assistance equipment.

INDEX TERMS Soft pneumatic elbow pad, smart campus environment, sEMG and RMS analysis, mechanical analysis, portable design.

I. INTRODUCTION

With the growth of age and the development of chronic health problems, the difficulties of doing daily work are becoming more and more common. Many problems will be caused such as therapeutic drugs, making use of a cane, cognitive adaptation, leaving school and quitting one's job. People rarely allow disablement to take its course without efforts to retard or stop the process. There are two ways to operate the method: one is to increase one's ability by improving one's physical or mental ability, the other is to reduce demand by reducing the physiological and psychological needs of a task [1]. Assistance equipment is acted directly on the patient and this method solves physical, psychological or social function problems through physical rehabilitation.

In recent years, wearable power equipment has become a hot topic which involves many related techniques including robotics, human engineering, mechanics, control engineering, medicine and rehabilitation. The wider meaning of power assisted system is to add an external source of power to the system, which makes the system add a certain multiplier to the external force. In the past, people paid more attention to the development of military and engineering. However, with the improvement of infrastructure and stable social environment, people put more focus on the improvement of human beings. With the continuous development of science and technology, this technology gradually step towards human itself, smart campus, medical as well as civilian.

Therefore, many scholars have studied many aspects of the assistance equipment, such as for the elbow, forearm, wrist, upper arm, ankle-foot, finger, knee and shoulder. There are many kinds of actuation technologies for elbow assisted, such as motor [2-4], cable [5-7], hydraulic [8-11] and pneumatic [12-18]. Several equipment which can generate

This article has been accepted for publication in a future issue of this journal, but has not been fully edited. Content may change prior to final publication. Citation information: DOI 10.1109/ACCESS.2018.2852757, IEEE Access

force to assist elbow movement has been put into the market such as SUITS *et al.* However, the assistance equipment at the current can be divided into two categories: (1) the utility model adopts the mechanism to support the power assisted part by means of supporting type. Most of them are made of rigid materials with low compliance and flexibility such as titanium alloy [19]; (2) the using of artificial muscle to stretch for power support part by means of stretching type. Most of them have good flexibility, but they occupy a lot of joint movement space. In the last five years, many scholars have been attracted by the advantages of soft robots [20-23]. These robots which are made of flexible and extensible material exhibit better safety and adaptability than rigid robots in structured and unstructured environment during the working [24]. Obtaining accurate dynamics is conducive to in-depth research and controller design [25-30], but this problem is not in the research scope of this paper.

According to the literature review, the home-made soft pneumatic elbow pad (For the readability of the paper, we call it SPEP for short in this paper) system is presented in smart campus platform to help students finish their daily life. Therefore, the problem of lightweight structure and flexible processing technologies in rigid mechanism design is no longer considered. In this system, the bending sensor (FLEX45, Spectrasymbol Inc., UT, USA), air pressure sensor (40PC150G2A, Honeywell Inc., NJ, USA) and force sensor (FSR®406, Interlinkelectronics Inc., CA, USA) are needed to make the SPEP better used. The SPEP will give us another way to design a better and more comfortable assistance equipment. The contents of this paper is organized as follows: Section Ⅱ introduces the fabrication technology of SPEP. In Section Ⅲ, the components of SPEP system are simply described. Meanwhile, bending sensors and force sensors of SPEP are used to find main characteristics. The tests results are given to verify the effectiveness of SPEP and the results of those tests are discussed in Section Ⅳ. In Section Ⅴ, the designed portable backpack and the control system of SPEP is designed. Finally, we make a concise conclusion and main contribution of this paper is described in Section Ⅵ.

II. FABRICATION OF SOFT PNEUMATIC ELBOW

The SPEP is made up of soft material (Dragon Skin FX-Pro, Smooth-on Inc., PA, USA). The proposed SPEP is a synthesis of soft and stretchable pneumatic actuator though using shape deposition manufacturing approach. The complete set of moulds which include base mould, chamber moulds, segmented blocks and cover mould, as shown in Fig. 1, are fabricated by a 3D printer (Creator-Pro, Flashforge Inc., Zhejiang, China) with a 1.75 mm diameter polylactic acid filament.

The fabrication procedure of SPEP is straightforward and can be described in Fig. 2. Briefly, the SPEP fabrication procedure contains: 1) the segmented blocks, the chamber moulds and the base mould are assembled together, as shown in Fig. 2(a); 2) the silicone rubber (Part A and Part B) is pre-mixed equal weights in a glass container and a wooden stirrer is used to mix thoroughly for 2 minutes. Then the mixed silicone rubber is placed in vacuum equipment (RH025N, Hokaido Inc., Nanjing, China) for degassing; 3) after degassing, the mixture of silicone rubber is carefully poured into the assembled base mould and cover mould. Furthermore, a fiber cloth and bending sensor are placed onto one surface of cover mold. An air tube (diameter: 6mm) is plugged at one side. Then, they are solidified for 6 hours at room temperature, as shown in Fig. 2(b) and Fig. 2(c); 4) when the mixture of silicone rubber is fully solidified, the two most important parts of SPEP are completed. After the two parts are demoulded, they are integrated together, as shown in Fig. 2(d).

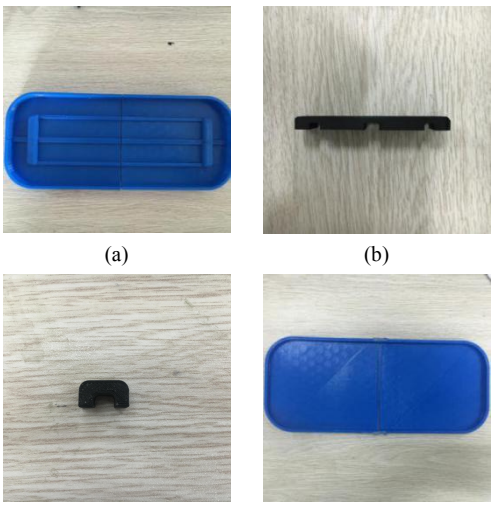

FIGURE 1. Schematic diagram of the moulds: (a) base mould, (b) chamber moulds, (c) segmentation blocks, (d) cover mould.

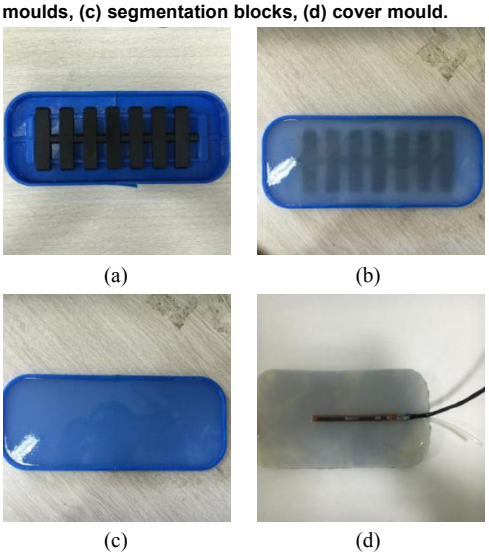

FIGURE 2. The fabrication procedure of SPEP: (a) assemble the bottom mould, (b) the bottom mold is injected with mixed silicone rubber, (c) the cover mold is injected with mixed silicone rubber, (d) combine two parts of SPEP with silicone rubber.

When the complete SPEP is prepared, its bending capacity is checked with compressed air, the test result is shown in Fig.

This article has been accepted for publication in a future issue of this journal, but has not been fully edited. Content may change prior to final publication. Citation information: DOI 10.1109/ACCESS.2018.2852757, IEEE Access

3. The structure of SPEP is a long trunk-like with a series of connected internal chambers. It can cause the structure to transform into a cured configuration with the inflation of gas. The structure diagram of SPEP is presented in Fig. 4. Fig. 4(a) shows the schematic diagram of the SPEP structure at uninflated state. When the SPEP expands, the top surface and side surfaces of each chamber extend, whereas the bottom surface is not extendible due to the constraint of the fabric cloth. So it leads to overall bending and it can be clearly expressed in Fig. 4(b).

FIGURE 3. The schematic diagram of SPEP filled with compressed air.

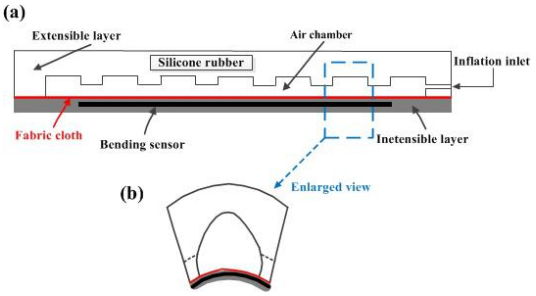

FIGURE 4. The SPEP structure diagram: (a) schematic diagram of the SPEP structure, (b) the schematic diagram of chamber expansion.

Ⅲ. HARDWARE EQUIPMENT

Based on the SPEP shown in Fig. 3, a stable and reliable system is developed. The schematic diagram of the system is presented in Fig. 5.

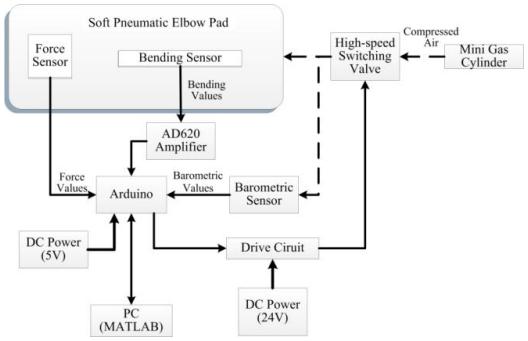

FIGURE 5. The schematic diagram of hardware for SPEP.

The Arduino Mega 2560 is chosen as the core of the SPEP controller and it is suitable for users with a large number of IO interfaces. Two 2-way solenoid valves (V1B02-BW1, Mead Fluid Dynamics Inc., IL, USA, response time: 10ms) are used. The AD 620 amplifier (Wheatstone bridge) is adopted to adjust the output voltage of bending sensor. Both 2-way solenoid valves and AD 620 amplifier need to be powered by DC power. One air pressure sensor is used to measure the air pressure of SPEP. The force sensor and bending sensor are used to measure the force values and bending values of SPEP when inflated pneumatically. Also , their performance has been tested and verified [31-34]. The designed algorithms are executed in Arduino Mega 2560. Through the MATLAB program in the host computer, the sensor data is collected by Arduino Mega 2560, processed and shown in real-time on PC. The communication between the Arduino Mega 2560 and the PC is wired. In the process of acquisition and processing, the low-pass filter is designed in MATLAB. These work has been completed in [33] and this paper focuses on the following research.

A. AIR PRESSURE VS. BENDING

Firstly, the meaning of some symbols is clearly explained to make the readers understand.

p	Air pressure of chamber	unit: kPa
u	Output voltage of air pressure sensor	unit: V
b	Bending angle of SPEP	unit: V

The air pressure sensor transmits pressure value p in SPEP to Arduino Mega 2560 as analog voltage and the relationship can be obtained with (1). Variable b can be acquired from Arduino Mega 2560.

$$p = \frac{15000u}{14.5 \times 4.5} \tag{1}$$

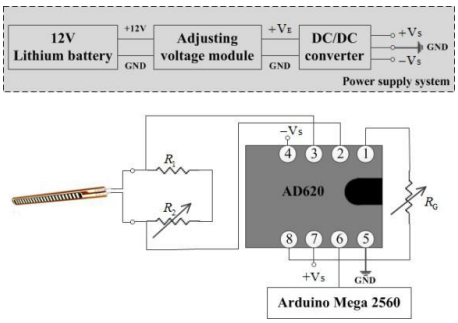

FIGURE 6. The complete signal amplification circuit used for bending sensor.

The bending characteristics of SPEP need to be measured. The bending sensor needs a suitable signal amplifying circuit which can output small variation signal in bending process to work effectively and it has a range of about 5~10kΩ. The AD 620 chip is adopted in the Wheatstone half bridge circuit. A complete bending sensor signal amplification circuit which is low-cost and easy to be fabricated is presented in Fig.6. This includes five important components: 1) a 12V lithium battery is energized to provide enough power; 2) a adjusting voltage module (input voltage: 3~30V, output voltage: 1.15~25V) is adopted to ensure a stable voltage output (+VE/GND: 5V); 3) to obtain the required dual output voltage (±VS/GND: ±12V), a DC/DC converter is used; 4) in the whole circuit, a variable resistor (R_2: 0~20kΩ) is needed to balance bending sensor resistance and adjust input voltage for AD620; 5) a constant

This article has been accepted for publication in a future issue of this journal, but has not been fully edited. Content may change prior to final publication. Citation information: DOI 10.1109/ACCESS.2018.2852757, IEEE Access

resistor (R_1: 10kΩ) is selected to implement bridge-arm circuit.

As the aforementioned, the SPEP can be bent when inflated pneumatically. Further, the explicit relationship between the air pressure values and the bending values needs to be discovered for SPEP use. The flexion and extension motion of SPEP can be described by the variable resistance of the bending sensor, as shown in Fig. 7(a). In the A-B segment, the resistance of bending sensor and the SPEP body did not show bending obviously when the air pressure in SPEP increased. In the B-C segment, the chambers of SPEP and the body begin to bend with the increase of SPEP internal air pressure. The C-D segment represents the normal using of SPEP. In the process of deflation, the gas in SPEP will not be discharged instantaneously, so the bending value has no obvious decrease in the D-E segment. The chambers with filled gas gradually regain its original shape along with the deflation continues, which is described by E-F segment. Due to the relaxation characteristic of bending sensor, the F-A segment is generated. After deflation, there is a small amount of residual gas in the SPEP. Therefore, the value of the air pressure sensor is not zero. Since the voltage range of the Arduino analog output is 0~5V, the initial bending value is set to 2.18V by adjusting signal amplifier circuit. The SPEP is filled with different air pressure values (10kPa, 20kPa, 30kPa, 40kPa, 50kPa, 60kPa and 70kPa). The average values of the five tests under each air pressure are described in Fig. 7(b). The results showed manifest that the pressure value of 50kPa can bring bending value which is close to the maximum value. Also, the SPEP bending values do not increase with the increasing air pressure values after 50kPa.

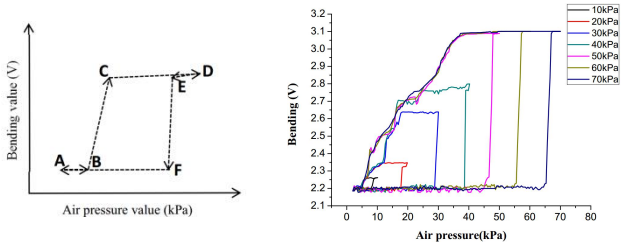

(a) (b)

FIGURE 7. Schematic diagram of SPEP bending characteristics: (a) diagram of SPEP characteristics (bending and releasing), (b) the test results in different air pressures.

B. AIR PRESSURE VS. FORCE

The force tests after wearing a SPEP is presented to quantify the SPEP performance where the force sensor of FSR®406 is used to record the contact force between the arm and SPEP, as shown in Fig. 8(a). The meaning of some symbols in this part is also explained to make the reader understand.

R_M	Pull-down resistor	unit: kΩ
V_{OUT}	Output voltage of force sensor	unit: V
V_{CC}	Input voltage of force sensor	unit: V
R_{FSR}	Resistance value of force sensor	unit: kΩ
F_{SPEP}	Force value provided by SPEP	unit: N

Similar to the bending sensor, the principle of the force sensor is that the change in the external pressure causes a change in the resistance value, and the outward appearance is shown in Fig. 8(a). A suitable signal amplifying circuit which contains a pull-down resistor (R_M: 5.1kΩ) is also presented in Fig. 8(b) and 8(c). For pressure and voltage conversion, the force sensor is tied to a measuring resistor in a voltage divider and the output is described by (2). According to (2), the resistance value of force sensor (R_{FSR}) can be obtained in (3). Previous results show that the output voltage increase with increasing forces and the resistance value of force sensor (R_{FSR}) is nonlinear with the force value[33]. In order to find out the characteristic curve of the force sensor, the weight group is used to calibrate the force points, as shown in Table Ⅰ.

$$V_{OUT} = \frac{R_M V_{CC}}{(R_M + R_{FSR})} \tag{2}$$

$$R_{FSR} = \frac{R_M (V_{CC} - V_{OUT})}{V_{OUT}} \tag{3}$$

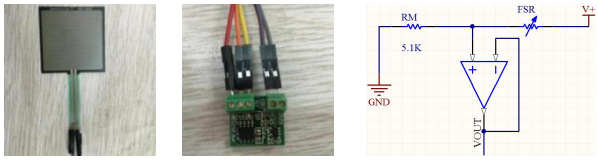

(a) (b) (c)

FIGURE 8. The signal amplification circuit and force sensor: (a) force sensor of the FSR®406, (b) the complete signal amplification circuit, (c) schematic diagram of signal amplification circuit.

TABLE Ⅰ

Force Values Corresponding to Different Resistance Values

Force value (gf)	R_{FSR} (kΩ)	Force value (gf)	R_{FSR} (kΩ)
800	3.01	2000	0.88
1000	2.28	2200	0.78
1200	1.78	2400	0.71
1400	1.49	2600	0.64
1600	1.19	2800	0.51
1800	1.09	3000	0.46

A suitable fitting curve is obtained with Matlab (Mathworks, Natick, MA, USA) based on the data, as shown in Fig. 9. The equation after fitting is presented in (4).

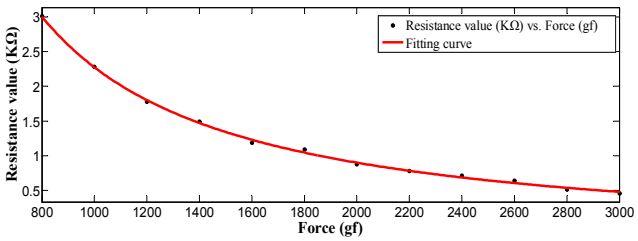

FIGURE 9. The schematic diagram of fitting curve.

$$R_{FSR} = ax^b + c \tag{4}$$

Where x represents the pressure value; $a \in [766.8, 1.32e+04]$, $b \in [-1.289, -1.008]$ and

This article has been accepted for publication in a future issue of this journal, but has not been fully edited. Content may change prior to final publication. Citation information: DOI 10.1109/ACCESS.2018.2852757, IEEE Access

$c \in [-0.4267, -0.03524]$ represent coefficients, respectively. When the parameters a, b and c are selected at 6984, -1.148 and -0.231 respectively, the (4) becomes the form of (5) and the average fitting error of eight results is 0.929%.

$$R_{\mathrm{FSR}} = 6984x^{-1.148} - 0.231 \qquad (5)$$

The force sensor is placed on the surface of one end of the SPEP to obtain the force provided (F_{SPEP}), as shown in Fig. 10(a). In order to wear SPEP more easily, the elastic bandage protector is used to fix it tightly on the elbows, as shown in Fig.13. Meanwhile, this ensures that the pressure sensor has the same initial value. The SPEP is also filled with different air pressure values (10kPa, 20kPa, 30kPa, 40kPa, 50kPa, 60kPa and 70kPa). Five tests are also conducted for different air pressure values. The results presented in Fig. 10(b) manifest that the SPEP force values increased with increasing the air pressure values. The force values of SPEP provided after 50kPa are obviously increased. However, through a large number of tests, it can be found that when the air pressure is higher than 70kPa, the SPEP has obvious plastic deformation, which is harmful to its structure and seriously affects the service life of SPEP. According to the aforementioned tests, all the following tests of SPEP are performed based on air pressure for 70kPa which the bending value and force value are 3.1V and 9.22N, respectively.

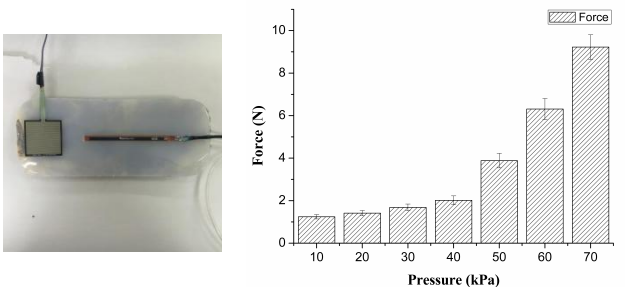

(a) (b)

FIGURE 10. Force test results: (a) the SPEP diagram with force sensor, (b) the force values of SPEP when the air pressure for 10kPa, 20kPa, 30kPa, 40kPa, 50kPa, 60kPa and 70kPa.

IV. EXPERIMENTAL EVALUATION

A. SEMG SIGNAL ANALYSIS

The muscle strength and activation of the human body are different, so the sEMG signals of different people are different at the same time. In order to verify the validity, only one object is selected to carry out several groups of experiments. The two acquisition channels (the biceps brachii and the triceps brachii) are used in the test subject. The effective range of sEMG is below 500Hz and the frequency of hardware acquisition is 1024Hz. The combination of low pass filter and first order median filtering are used in the signal processing engineering.

In this part of the collection, two common states of the elbow joint are tested. One is the elbow flexion and elbow extension, and the other is elbow relaxation. In the elbow flexion and extension state, the test time is 8min, and the test subject is required to complete 8 sets of lifting and lowering. When the elbow is relaxed, the test time is also 8min, and the test object is only required to complete the natural state of the elbow. Each action is tested 5 times with holding a 3kg weight in their hand. After each measurement, the test object rest 30min in order to ensure the effectiveness of the experiment. In the 8 minutes of the test object movement, we intercept the middle 3.5 minutes for analysis, as shown in the following. Muscular effort is estimated from RMS of the sEMG activity of the main muscle involved in performing elbow movements, i.e. the biceps brachii and the of triceps brachii.

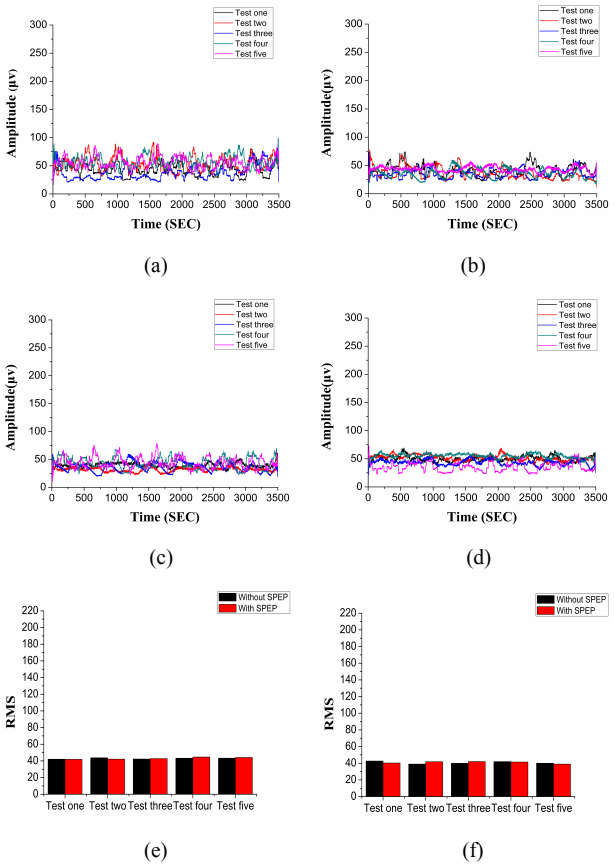

FIGURE 11. The diagram of sEMG and RMS of sEMG under the elbow relaxation: (a) the sEMG of biceps brachii without SPEP, (b) the sEMG of triceps brachii without SPEP, (c) the sEMG of biceps brachii with SPEP, (d) the sEMG of triceps brachii with SPEP, (e) the RMS of sEMG in the biceps brachii without SPEP and with SPEP, (f) the RMS of sEMG in the triceps brachii without SPEP and with SPEP.

From Fig. 11(a), (c) and (e), it can be concluded the sEMG of biceps brachii without SPEP and with SPEP are not changed. The range of the RMS of sEMG in biceps brachii without SPEP is from 42.08 to 43.75. The range of the RMS of sEMG in biceps brachii with SPEP is from 41.89 to 44.64. There is no obvious change in the RMS values of sEMG. From Fig. 11(b), (d) and (f), it can be concluded the sEMG of triceps brachii without SPEP and with SPEP are not changed. The range of the RMS of sEMG in triceps brachii without SPEP is from 39.01 to 42.69. The range of the RMS of sEMG in triceps brachii with SPEP is from 39.01 to 42.01. There is also no obvious change in the RMS values of sEMG.

This article has been accepted for publication in a future issue of this journal, but has not been fully edited. Content may change prior to final publication. Citation information: DOI 10.1109/ACCESS.2018.2852757, IEEE Access

It can be seen that wearing SPEP does not change the activity of the muscle during the relaxation process. By consulting the wearers, it shows that wearing SPEP is painless and comfortable.

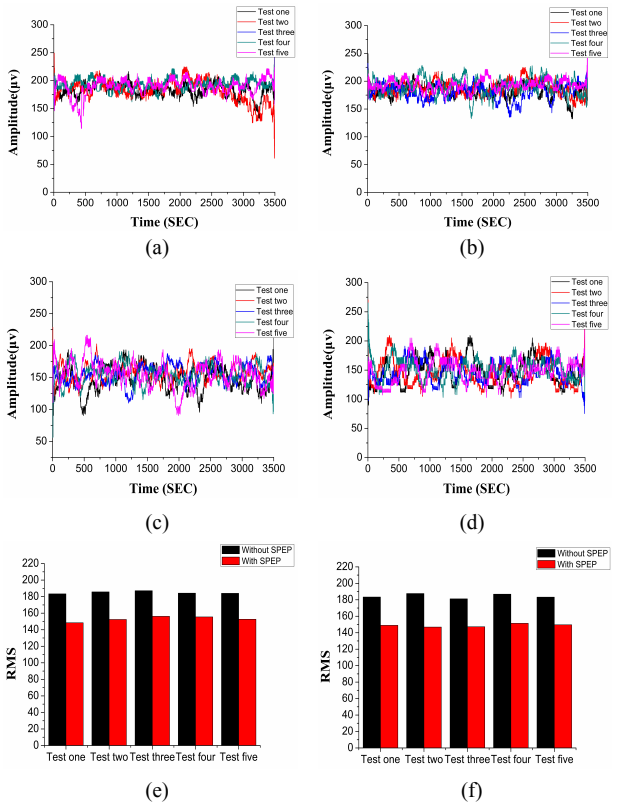

FIGURE 12. The diagram of sEMG and RMS of sEMG under the elbow flexion and extension: (a) the sEMG of biceps brachii without SPEP, (b) the sEMG of triceps brachii without SPEP, (c) the sEMG of biceps brachii with SPEP, (d) the sEMG of triceps brachii with SPEP, (e) the RMS of sEMG in the biceps brachii without SPEP and with SPEP, (f) the RMS of sEMG in the triceps brachii without SPEP and with SPEP.

From Fig. 12(a), (c) and (e), it can be concluded that the sEMG of biceps brachii are significantly reduced under the elbow flexion and extension by wearing SPEP. The range of the RMS of sEMG in biceps brachii without SPEP is from 183.35 to 187.19. The range of the RMS of sEMG in biceps brachii with SPEP is from 148.40 to 156.18. The SPEP had a significant effect on the biceps brachii and the average of RMS of sEMG decreases by 18.72% during flexion and extension. From Fig. 12(b), (d) and (f), it can be concluded the sEMG of triceps brachii which also significantly altered under the elbow flexion and extension by wearing SPEP. The range of the RMS of sEMG in triceps brachii without SPEP is from 181.17 to 187.65. The range of the RMS of sEMG in triceps brachii with SPEP is from 146.86 to 151.43. The results show that compared with the absence of SPEP, the average of RMS of sEMG in the triceps brachii decreases by 19.32%. It can be seen that wearing SPEP can reduce the activity of the muscle under flexion and extension. Meanwhile, according to the conclusion mentioned above, it can be shown that SPEP can also save power for the elbow under flexion and extension.

B. MECHANICAL ANALYSIS

In order to specifically get the effect of SPEP after wearing, the following analysis is carried out. The meaning of some symbols is exhibited in the following.

F_b	The force produced by the biceps brachii and brachial	unit: N
F_p	The gravity of the object in hand	unit: N
F_w	The total gravitational force produced by the forearm and the palm	unit: N
F_j	The force of olecranon	unit: N
L_1	The distance between the center of olecranon and the force of F_b	unit: cm
L_2	The distance between the center of gravity of forearm and center of olecranon	unit: cm
L_3	The distance between the palm of human body and the center of olecranon	unit: cm
L	The height of the human body	unit: cm
L_{SPEP}	The distance between the center of human olecranon and the force of F_{SPEP}	unit: cm
W	The weight of human body	unit: kg

Before doing the following analysis, the forearm length of Chinese adults need to be known. According to human dimensions of Chinese adults (GB-10000-88), the average height of 15-60 year old Chinese men and women data can be got, as shown in Table Ⅱ.

TABLE Ⅱ
Chinese Height

Average age	Percentile	Male height(cm)	Female height(cm)
15-60 years old	1	154.3	144.9
	5	158.3	148.4
	10	160.4	150.3
	50	167.8	157.0
	90	175.4	164.0
	95	177.5	165.9
	99	181.4	169.7

Meanwhile, the body ideal weight and forearm weight can be obtained by (6). In the process of elbow flexion, the main force is produced by the biceps brachii and brachial. Due to each person has different arm widths, we assume that the L_1 is 5cm as shown in Fig. 13.

$$\begin{aligned} F_W &= (0.008W + 0.026W) \times 10 = 0.34W \\ L_2 &= L \times (0.506 - 0.429) = 0.077L \\ L_3 &= L \times (0.25 - 0.0545) = 0.1955L \end{aligned} \tag{6}$$

Where, $W \in [L-110, L-100]$. In this paper, in order to facilitate calculation, the acceleration of gravity is set at 10N/kg.

When the weight is held in the hand, the counter force of the elbow flexion can be calculated by the simplified free limb. At the beginning, the body is required to hold lighter weights. As the working process continues, hand weight increases as well. The weights of 0.5kg, 1kg, and 2kg are presented to achieve the requirements of the analysis. Due

This article has been accepted for publication in a future issue of this journal, but has not been fully edited. Content may change prior to final publication. Citation information: DOI 10.1109/ACCESS.2018.2852757, IEEE Access

to W which has a certain range, there are also a certain range of F_b and F_j . In the analysis, subjects are required to bend their elbows at 90 degrees. The balance equation provides that the torque and force acting on the elbow should be zero. The force of the olecranon can be calculated by (7) and (8).

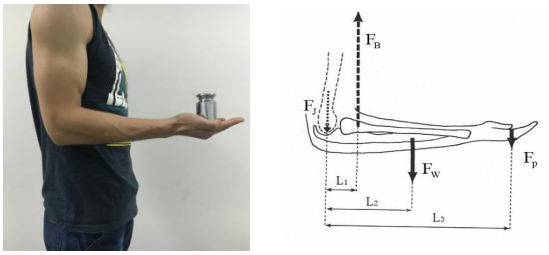

(a) (b)

FIGURE 13. Diagram of joint reaction force during elbow flexion. (a) the diagram of elbow bending, (b) a simplified model during elbow flexion.

$$\sum \mathbf{M}(\mathrm{J}) = 0$$
$$L_2 \cdot F_w + L_3 \cdot F_p - L_1 \cdot F_b = 0 \quad (7)$$
$$F_b = \frac{L_2 \cdot F_W + L_3 \cdot F_p}{L_1}$$

$$\sum \mathbf{F} = 0$$
$$F_b - F_j - F_w - F_p = 0 \quad (8)$$
$$F_j = F_b - F_w - F_p$$

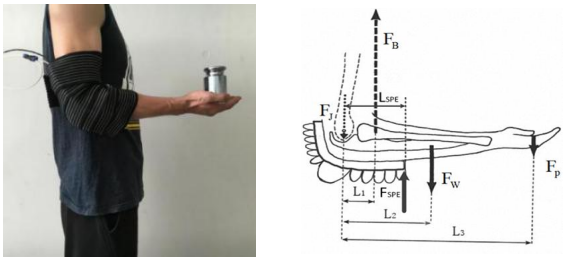

(a) (b)

FIGURE 14. Diagram of joint reaction force during elbow flexion when wearing SPEP. (a) the diagram of elbow bending, (b) a simplified model during elbow flexion.

Next, the human body with SPEP is analyzed to verify the SPEP which can reduce the force of olecranon and save the force of muscle, as shown in Fig. 14(a). When the subjects wear SPEP, they are also required to bend their elbows by 90 degrees. It supports force F_{SPEP} by wearing SPEP and the distance from the center of human olecranon (L_{SPEP}) are shown in Fig. 14(b). Then the (7) and (8) should be changed as shown in (9) and (10). According to the SPEP state of wearing, the value of L_{SPEP} can be measured which is set to 17(cm) in the article. The force value (F_{SPEP}) is 9.22N.

$$\sum \mathbf{M}(\mathrm{J}) = 0$$
$$L_2 \cdot F_w + L_3 \cdot F_p - L_1 \cdot F_b - L_{SPEP} \cdot F_{SPEP} = 0 \quad (9)$$
$$F_b = \frac{L_2 \cdot F_w + L_3 \cdot F_p - L_{SPEP} \cdot F_{SPEP}}{L_1}$$

$$\sum \mathbf{F} = 0$$
$$F_b + F_{SPEP} - F_j - F_w - F_p = 0 \quad (10)$$
$$F_j = F_b + F_{SPEP} - F_w - F_p$$

In the subjects, one male and one female were selected to be as test items. Each subject was calculated 5 times under different hand load conditions. The error bar marked in the figure show the standard deviation of the five results of each test. The average results shown in Fig. 15 that the elbows can be effectively assisted in working process. When male and female wear SPEP, the average forces of the biceps brachii and the brachialis decrease about 31.33N and the average forces of the olecranon decrease about 22.12N. The results of the analysis demonstrate that the SPEP can help people with the olecranon joint and muscle section of the elbow. Maybe, these results can provide a pathway for rehabilitation of patients with elbow joint injuries.

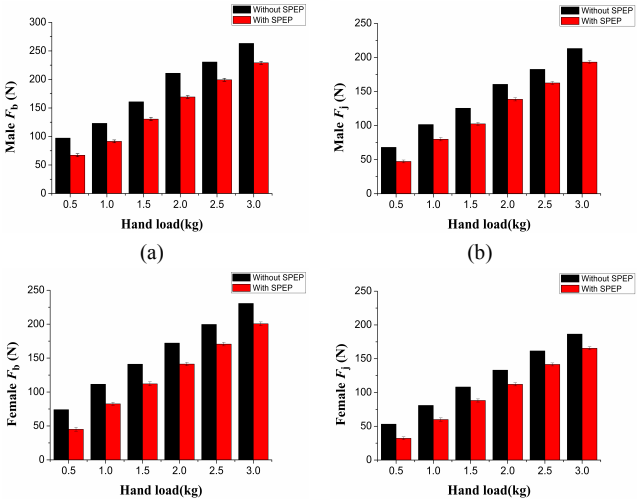

FIGURE 15. The force of the biceps and the olecranon. (a) the F_b of male with and without SPEP, (b) the F_j of male with and without SPEP, (c) the F_b of female with and without SPEP, (d) the F_j of female with and without SPEP.

V. PORTABLE DESIGN

In order for SPEP to better help people in the process of assisting, a portable is designed as shown in Fig. 16.

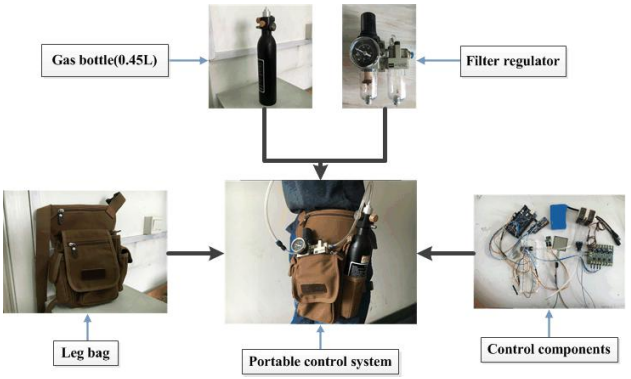

FIGURE 16. The schematic diagram of portable control system.

The hardware and mini gas cylinder are arranged in the leg bag. Under the condition of 70kPa pressure, the mini gas

This article has been accepted for publication in a future issue of this journal, but has not been fully edited. Content may change prior to final publication. Citation information: DOI 10.1109/ACCESS.2018.2852757, IEEE Access

cylinder can finish the 600 times inflating and bleeding for SPEP. The SPEP is a soft structure that does not affect the natural movements of the humans' elbows when it is not driven. This is also the advantage compared with the rigid structure. On the other hand, we have designed the security control mode. When the pressure of the air chamber is higher than the safe pressure, the control system which ensures the air pressure of SPEP in a safe range will forcibly close the air inlet and open the air outlet to release the air pressure. At the same time, the air pressure sensor and bending sensor are used again which were used as dual channel switches. Then, the PID controller is designed to regulate the pressure values. The execution of the SPEP can be described as the following Algorithm 1.

Algorithm 1 SPEP Control

1: **for** i=0, i≤max iterations, i++
2: **if** b<desired bending value **then**
3: Execute motion
4: **else if** p<desired barometric value **then**
5: Execute motion (a PID controller is used to adjust PWM values)
6: **else** Maintain motion
7: SPEP releases

VI. CONCLUSION

The main contribution of this paper is that a new-type of soft pneumatic elbow pad which are based on low-cost and easy-to-procure has been presented and three simple commercial sensors (bending sensor, air pressure sensor and force sensor) are adopted. The SPEP is fabricated by using shape deposition manufacturing approach with silicone rubber. Then, the air pressure values vs. bending values and force values wearing of SPEP vs. air pressure values are presented. The pressure value of 50 kPa can maximize the bending value. It means that the SPEP bending does not change when the pressure is higher than 50 kPa. However, the SPEP force values increased with increasing the air pressure values. When the SPEP is charged with 70kPa, the SPEP can output the force of 9.22N. The two important relationships are obtained and applied to SPEP. Therefore, in order to verify the effectiveness of designed SPEP, two analysis ways are presented. Through RMS analysis of the sEMG, the first method demonstrated that wearing a SPEP does not change muscle activity when it is not working, and it can reduce muscle activity during the flexion and extension of the elbow. The second approach is to use wearable analysis by calculating the simplified free limb. In the process of analysis, subjects are asked to bend their elbows at 90 degrees. The balance equation provides that the torque and force acting on the elbow should be zero. Through the analysis, we can conclude when male and female wearing SPEP, the forces of the biceps brachii and the branchialis decreased by 31.33N and the forces of the olecranon decreased by 22.12N. Finally, we design a portable wearable backpack for SPEP control system and energy system. Meanwhile, the PID controller is added to the control system.

The emergence of SPEP will bring a few ideas for who study in the field of assistance or rehabilitation. The design idea of SPEP is to put actuators, controllers and power sources on the body and providing the wearer with power or rehabilitation. The light assistance equipment or rehabilitation products have not yet appeared on the market. Therefore, this design will walk out the smart campus environment. In the end, SPEP can greatly fill the gap in the market and facilitate for more families. In our future work, we plan to analyze the internal structure changes of SPEP under the inflatable condition. We also plan to establish a reasonable model for SPEP. By modeling and analyzing the cavity structure of SPEP, a better structural optimization design method is found for the field of soft assistance equipment.

ACKNOWLEDGMENT

The support of Chen Yang (processing data), Yao Sun (structural design), Hui Yang (circuit design), Chaoqun Xiang (result analysis) and Lina Hao (technical guidance and reviewed this manuscript) is acknowledged. In addition, the authors would also like to sincerely thank the editors and reviewers for their pertinent comments and guidance that helped this article become more professional and precise.

REFERENCES

[1] L. M. Verbrugge, C. Rennert, and J. H. Madans, "The great efficacy of personal and equipment assistance in reducing disability," *American journal of public health*, vol. 87 no. 3, pp. 384-392, 1997.
[2] R. A. R. C. Gopura, K. Kiguchi, and Y. Li, "SUEFUL-7: a 7DOF upper-limb exoskeleton robot with muscle-model-oriented EMG-based control", in *IEEE/RSJ International Conference on Intelligent Robots and Systems*, St. Louis, MO, USA, 2009, pp. 1126–1131.
[3] T. Otsuka, K. Kawaguchi, H. Kawamoto, and Y. Sankai, "Development of upper-limb type HAL and reaching movement for meal-assistance," in *IEEE International Conference on Robotics and Biomimetics*, Karon Beach, Phuket, Thailand, 2011, pp. 883–888.
[4] Y. Hasegawa and S. Oura, "Exoskeletal meal assistance system (EMAS II) for progressive muscle dystrophy patient," in *IEEE International Conference on Rehabilitation Robotics*, Besacon, France, 2011, pp. 1–6.
[5] L. Tappeine, E. Ottaviano, M. L. Husty, "A Cable-Driven Robot for Upper Limb Rehabilitation Inspired by the Mirror Therapy", *Computational Kinematics. Springer, Cham*, pp. 174-181, 2018.
[6] L Zhou *et al.*, "Modeling and design of a spring-loaded, cable-driven, wearable exoskeleton for the upper extremity," *Modeling Identification & Control,* vol. 36, no. 3, pp. 167–177, 2015.
[7] Y Mao *et al.*, "Human movement training with a cable driven ARm EXoskeleton (CAREX)," *IEEE Transactions on Neural Systems and Rehabilitation Engineering*, vol. 23 no. 1, pp. 84-92, 2015.
[8] A Otten *et al.*, "LIMPACT: A hydraulically powered self-aligning upper limb exoskeleton," *IEEE/ASME transactions on mechatronics*, vol 20 no 5, pp. 2285-2298, 2015.
[9] T. Lenzi, S. De Rossi, N. Vitiello, A. Chiri, S. Roccella, F. Giovacchini, F. Vecchi, and M.C. Carrozza, "The neuro-robotics paradigm: NEURARM, NEUROExos, HANDEXOS," in *Conf. Proc. Annu. Int. Conf. IEEE Eng. Med. Biol. Soc.*, Minneapolis, MN, USA, 2009, pp. 2430–2433.
[10] N. Vitiello, T. Lenzi, S. Roccella, S. Marco, M. De Rossi, E. Cattin, F. Giovacchini, F. Vecchi, and M.C. Carrozza, "NEUROExos: A powered elbow exoskeleton for physical rehabilitation," *IEEE Trans. Robot*. vol. 29, no. 1, pp. 220–235, 2013.
[11] C. Pylatiuk, A. Kargov, I. Gaiser, T. Werner, S. Schulz, and G. Bretthauer, "Design of a flexible fluidic actuation system for a hybrid elbow orthosis," in *IEEE International Conference on Rehabilitation Robotics*, Kyoto, Japan 2009, pp. 167–171.

[12] K. Y. Hong *et al.*, "A soft exoskeleton for hand assistive and rehabilitation application using pneumatic actuators with variable stiffness," in *IEEE International Conference on Robotics and Automation IEEE*, Seattle, WA, USA, 2015, pp. 4967-4972.
[13] T. Noda *et al.*, "Development of an upper limb exoskeleton powered via pneumatic electric hybrid actuators with bowden cable," in *IEEE/RSJ International Conference on Intelligent Robots and Systems*, Chicago, IL, USA, 2014, pp. 3573-3578.
[14] L. W. Lee. "Exoskeleton apparatus driven by pneumatic artificial muscle with functions of upper limb assist and rehabilitation training," *U.S. Patent Application*, vol. 15, pp. 485–486, 2017.
[15] T. Noritsugu, "Wearable power assist robot driven with pneumatic rubber artificial muscles," *Virtual Reality Enhanced Robotic Systems for Disability Rehabilitation*, pp. 235-250, 2016.
[16] H. Jitosho, F. Fujii, "A reference augmentation design for the adaptive control of a wearable assist robot powered by the McKibben actuator," in *IEEE International Conference on Systems, Man, and Cybernetics*, Banff, AB, Canada, 2017, pp. 1099-1104.
[17] T. Kosaki et al. "A pneumatic arm power-assist system prototype with EMG-based muscle activity detection," in *IEEE International Conference on Mechatronics and Automation*, Takamatsu, Japan, 2017,pp. 793-798.
[18] J. Klein, S. Spencer, J. Allington, J.E. Bobrow, D.J. "Reinkensmeyer, Optimization of a parallel shoulder mechanism to achieve a high-force, low-mass, roboticarm exoskeleton," *IEEE Trans. Robot*, vol. 26, no. 4, pp. 710–715, 2010.
[19] A. Yang *et al.*, "Optimum surface roughness prediction for titanium alloy by adopting response surface methodology", *Results in Physics*, no. 7, pp. 1046-1050, 2017.
[20] J. Bishop-Moser and S. Kota, "Design and modeling of generalized fiber-reinforced pneumatic soft actuators," *IEEE Trans Robot*, pp. 4967-4972, 2015.
[21] L. Guo *et al.*, "Soft pneumatic grippers embedded with stretchable electroadhesion", *Smart Materials and Structures,* vol. 27, no. 5, pp. 055006, 2018.
[22] C. Laschi, B. Mazzolai, and M. Cianchetti, "Soft robotics: Technologies and systems pushing the boundaries of robot abilities," *Nature*, vol. 1, no. 1, pp. eaah3690, 2016.
[23] D. Rus and M. T. Tolley, "Design, fabrication and control of soft robots," *Soft Robotics*, vol. 521, no. 7553, pp. 467-475, 2015.
[24] C. Laschi, B. Mazzolai, and M. Cianchetti, "Soft robotics: Technologies and systems pushing the boundaries of robot abilities," *Science Robotics*, vol. 1, no. 1, pp. 1-11, 2016.
[25] K. Cui and X. Qin. "Virtual reality research of the dynamic characteristics of soft soil under metro vibration loads based on BP neural networks". *Neural Computing and Applications*, vol. 29, no. 5, pp. 1233-1242, 2018.
[26] K. Cui and T. T. Zhao. "Unsaturated dynamic constitutive model under cyclic loading". *Cluster Computing*, vol. 20, no. 4, pp. 2869-2879, 2017.
[27] Y. G. Sun *et al.*, "Modified repetitive learning control with unidirectional control input for uncertain nonlinear systems", *Neural Computing and Applications*, pp. 1-10, 2017.
[28] Y. G. Sun *et al.*, "The nonlinear dynamics and anti-sway tracking control for offshore container crane on a mobile harbor", *Journal of Marine Science and Technology-Taiwan*, vol. 25, no. 6, pp. 656-665, 2017.
[29] C. Xiang *et al.,* "Variable stiffness Mckibben muscles with hydraulic and pneumatic operating modes", *Advanced Robotics,* vol. 30, no. 13, pp. 889-899, 2016.
[30] C. Xiang *et al.,* "The design, hysteresis modeling and control of a novel SMA-fishing-line actuator", *Smart Materials and Structures,* vol. 26, no. 3, pp. 037004, 2017.
[31] D. H. Kim, S. W. Lee, and H. S. Park, "Sensor evaluation for soft robotic hand rehabilitation devices," in *IEEE International Conference on Biomedical Robotics and Biomechatronics*, Singapore, Singapore, 2016, pp. 1220-1223.
[32] Y. Luo, Y. Shen, and N. Mohan, "Durable and cost-effective 3-D microforce sensor for musical tuning enhanced micro palpation of biological entities," *Sensors. IEEE*, pp. 1-4, 2013.
[33] X. Gao, Y.Sun, L. Hao, C. Xiang and H. Cheng, "A new type of soft pneumatic elbow," in *IEEE International Conference on Robotics and Biomimetics*, Macao, China, 2017, pp. 2681-2686.
[34] Y. Chen *et al.*, "An Ultrasensitive Flexible and Bending Sensor for Detecting Angle and Micro-force," *Advances in Comptuer Science Research*, vol.43, pp. 32-36, 2016.

Xifeng Gao was born in Shenyang city, China in 1990. He received the B.S. degree in Mechanical Design, Manufacturing and Automation from Hebei University of Technology, Tianjin, China in 2013, M.S. degree in Mechanical Engineering from Hebei University of Technology, Tianjin, China in 2016. He is current a Ph.D. candidate at Northeastern University, Shenyang, China. His research interests include modeling and control of artificial muscles especially in PAM, soft robotics and robot trajectory planning and system control.

Yao Sun was born in Harbin, China, in 1992. He received the B.S. degree in Mechanical Engineering and Automation from Northeastern University, Shenyang, China in 2015. He is currently a master graduate at the Northeastern University, Shenyang, China. His research interests include modeling and control of PAM and design of mechanical structure and drive system for wearable exoskeleton.

Lina Hao was born in Zhuanghe, China, in 1968. She received the B.S. degree in machinery design and manufacture from Shenyang Ligong University, Shenyang, China in 1989. M.S. degree in solid mechanics and Ph.D. degree in control theory and control engineering from Northeastern University, Shenyang, China in 1994 and 2001, respectively. Currently, she is a professor in Department of Mechanical Engineering and Automation in Northeastern University, China. Her research interests include robot system and intelligent control, intelligent structure and precision motion control system, pattern recognition and condition monitoring. Prof. Hao is selected as a hundred-level member in "Pacesetter Project" Liaoning province, China, a member of International Society of Bionic Engineering and a member of Chinese Association of Automation System Simulation Discipline and Robot Discipline Committee.

Hui Yang was born in Jinzhou, China, in 1987. He received the B.S. degree and M.S. degree in machinery design and manufacture from Liaoning Shihua University, Fushun, China in 2010 and 2013, respectively. He is currently a Ph.D. candidate at the Northeastern University, Shenyang, China. His research interests include modeling and control of PAM and compliance control of the bionic manipulator actuated by artificial muscles. He is a student member of IEEE and International Society of Bionic Engineering.

This article has been accepted for publication in a future issue of this journal, but has not been fully edited. Content may change prior to final publication. Citation information: DOI 10.1109/ACCESS.2018.2852757, IEEE Access

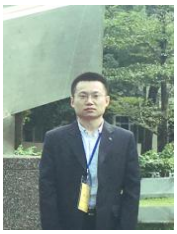

Yang Chen was born in Qitaihe city, China in 1988. He received the B.S. degree in mechanical engineering and automation from China University of Mining and Technology, Xuzhou, China in 2012, M.S. degree in mechatronic engineering from Northeastern University, Shenyang, China in 2014. He is currently a Ph.D. candidate at Northeastern University, Shenyang, China. His research interests include driving, modeling and control of artificial muscles especially in IPMC and SMA, and soft robotic hand. He is a student member of IEEE and International Society of Bionic Engineering.

Chaoqun Xiang obtained his BEng and MSc degree in Mechanical Design and Theory from Liaoning University of Technology (P.R. China) in 2009 and 2012 respectively. Dr. Xiang received his Ph.D. degree in Mechatronic Engineering from Northeastern University (P.R. China) in 2017. He was a visiting researcher in the Centre for Robotics and Autonomous System robotics at Salford University (UK). He is now working in Bristol Robotics Laboratory as research associate in Soft Robotics based in the University of Bristol (UK). His main research interests include bionic drivers of artificial muscles and intelligent control methods for soft robots.